



Design of robust differential microphone arrays with the Jacobi–Anger expansion [☆]



Liheng Zhao ^a, Jacob Benesty ^a, Jingdong Chen ^{b,*}

^aINRS-EMT, University of Quebec, 800 de la Gauchetiere Ouest, Suite 6900, Montreal, QC H5A 1K6, Canada

^bCenter of Intelligent Acoustics and Immersive Communications, Northwestern Polytechnical University, 127 Youyi West Rd, Xi'an, Shaanxi 710072, China

ARTICLE INFO

Article history:

Received 2 August 2015

Received in revised form 14 January 2016

Accepted 20 March 2016

Available online 31 March 2016

Keywords:

Differential microphone arrays (DMAs)

Robust DMAs

Beampattern

Beamforming

White noise gain

Directivity factor

First-order DMA

Second-order DMA

Third-order DMA

Jacobi–Anger expansion

ABSTRACT

Due to their small size, differential microphone arrays (DMAs) are very attractive. Moreover, they have been effective in combating noise and reverberation. Recently, a new class of DMAs of different orders have been developed with the MacLaurin's series and the frequency-independent patterns. However, the MacLaurin's series does not approximate well the exponential function, which appears in the general definition of the beampattern, when the intersensor spacing is not small enough. To circumvent this problem, we propose in this paper to approximate the exponential function with the Jacobi–Anger expansion. Based on this approximation and the frequency-independent Chebyshev patterns, we derive first-, second-, and third-order DMAs. Furthermore, in order to improve the robustness of DMAs against white noise amplification, we propose to use more microphones combined with minimum-norm filters. It is also shown that the Jacobi–Anger expansion is optimal from a mean-squared error perspective. Simulations are carried out to evaluate the performance of the proposed DMAs.

© 2016 Elsevier Ltd. All rights reserved.

1. Introduction

It is well known that noise and reverberation are detrimental to the speech quality and intelligibility. As a consequence, the performance of many applications, such as hands-free telecommunication and hearing aids, can be severely degraded. Over the past decades, approaches based on microphone arrays and beamforming techniques have been widely studied in the difficult context of noisy and reverberant environments [1–4]. Recently, methods based on differential microphone arrays (DMAs) have received a great deal of attention due to their small size and potential of high directivity factors [5–8]. As early as in the 1940s, DMAs of different orders were constructed and their anti-noise characteristics were analyzed [9,10]. Since then, a good amount of progress has been made. In [11,12], adaptive DMAs were developed to suppress spatially non-stationary noise. In [13], an approach based on sensor calibration was designed to increase DMAs' robustness against sensor mismatch, which may seriously damage their performance.

In [14], DMAs were used to estimate the noise power spectral density (PSD), and the spectral subtraction algorithm was then applied to suppress noise. In [15,16], approaches for the design of higher-order DMAs were developed. In [6,7], DMAs were systematically studied from a signal processing perspective. Specifically, the design, implementation, and performance analysis of DMAs were presented.

In [6,8], the exponential function, which appears in the general definition of the beampattern, was approximated with the MacLaurin's series; this led to the design of DMAs of different orders. It has been reported that DMAs based on the MacLaurin's series are capable of achieving high directivity factors. However, it has been observed that when the intersensor spacing is not very small, the MacLaurin's series is no longer a good approximation of the exponential function. As a result, the performance of DMAs is affected. To avoid this problem, we propose in this paper to use the Jacobi–Anger expansion to approximate the exponential function. We first derive the traditional¹ first-, second-, and third-order DMAs. Many simulation results show that the traditional DMAs with the Jacobi–Anger expansion significantly improve the directivity

[☆] This work was supported in part by the NSFC "Distinguished Young Scientists Fund" under Grant No. 61425005.

* Corresponding author.

E-mail address: jingdongchen@ieee.org (J. Chen).

¹ By traditional, we mean that the order of the DMA is equal to $M - 1$, where $M \geq 2$ is the number of microphones.

factor, but have the problem of white noise amplification, like any other approaches. To deal with this serious side effect, we derive robust DMAs by using more microphones combined with minimum-norm filters. It is shown that the robust DMAs with the Jacobi–Anger expansion improve the white noise gain considerably and, therefore, are more robust against any imperfections in the system. In comparison with DMAs based on the MacLaurin’s series, DMAs based on the Jacobi–Anger expansion perform better by giving higher directivity factors and white noise gains, confirming that the latter approximation is preferable in the derivation of DMAs. It is also shown that the Jacobi–Anger expansion is optimal from an MSE perspective.

The rest of this paper is organized as follows. In Section 2, some basic concepts of DMAs are introduced. In Section 3, frequency-independent patterns and the approximation based on the Jacobi–Anger expansion are presented. The traditional and robust first-, second-, and third-order DMAs are derived in Sections 4–6, respectively. Simulations are carried out to evaluate the performance of DMAs in Section 7, followed by our conclusions in Section 8.

2. Signal model, problem formulation, and definitions

We consider a source signal (plane wave), in the farfield, that propagates in an anechoic acoustic environment at the speed of sound, i.e., $c = 340$ m/s, and impinges on a uniform linear sensor array consisting of M omnidirectional microphones, where the distance between two successive sensors is equal to δ (see Fig. 1). The direction of the source signal to the array is parameterized by the azimuth angle θ . In this scenario, the steering vector (of length M) is given by

$$\mathbf{d}(\omega, \theta) = [1 \quad e^{-j\omega\tau_0 \cos \theta} \quad \dots \quad e^{-j(M-1)\omega\tau_0 \cos \theta}]^T, \quad (1)$$

where the superscript T is the transpose operator, $j = \sqrt{-1}$ is the imaginary unit, $\omega = 2\pi f$ is the angular frequency, $f > 0$ is the temporal frequency, and $\tau_0 = \delta/c$ is the delay between two successive sensors at the angle $\theta = 0$. The acoustic wavelength is $\lambda = c/f$.

In order to avoid spatial aliasing [3], which has the negative effect of creating grating lobes (i.e., copies of the main lobe, which usually points toward the desired signal), it is necessary that the inter-element spacing is less than $\lambda/2$, i.e.,

$$\omega\tau_0 < \pi. \quad (2)$$

The condition (2) easily holds for small values of δ and at low frequencies but not at high frequencies.

We consider fixed beamformers, such as DMAs [6,7,13,15,16], where the main lobe is at the angle $\theta = 0$ (endfire direction) and the desired signal propagates from the same angle. Our focus is on the design of different orders DMAs that are robust to white noise amplification. For that, a complex weight, $H_m^*(\omega)$, $m = 1, 2, \dots, M$, is applied at the output of each microphone, where the superscript $*$ denotes complex conjugation. The weighted outputs are then summed together to form the beamformer output as shown in Fig. 1. Putting all the gains together in a vector of length M , we get

$$\mathbf{h}(\omega) = [H_1(\omega) \quad H_2(\omega) \quad \dots \quad H_M(\omega)]^T. \quad (3)$$

Then, the objective is to design such a filter so that the array obeys a given DMA pattern.

The vector containing the microphone signals can be expressed as

$$\mathbf{y}(\omega) = [Y_1(\omega) \quad Y_2(\omega) \quad \dots \quad Y_M(\omega)]^T = \mathbf{d}(\omega, 0)X(\omega) + \mathbf{v}(\omega), \quad (4)$$

where $\mathbf{d}(\omega, 0)$ is the steering vector at $\theta = 0$ (direction of the source), $X(\omega)$ is the desired signal, and

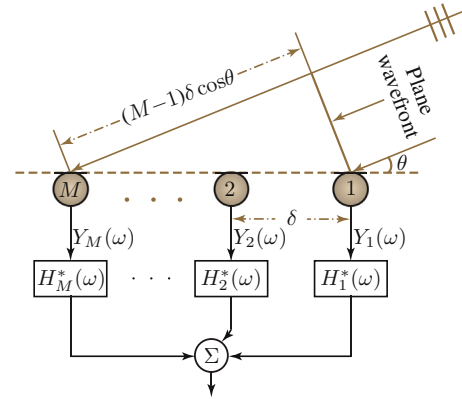


Fig. 1. A uniform linear microphone array with processing.

$$\mathbf{v}(\omega) = [V_1(\omega) \quad V_2(\omega) \quad \dots \quad V_M(\omega)]^T \quad (5)$$

is the additive noise signal vector.

The beamformer output is simply [4]

$$Z(\omega) = \mathbf{h}^H(\omega)\mathbf{y}(\omega) = \mathbf{h}^H(\omega)\mathbf{d}(\omega, 0)X(\omega) + \mathbf{h}^H(\omega)\mathbf{v}(\omega), \quad (6)$$

where $Z(\omega)$ is the estimate of the desired signal, $X(\omega)$, and the superscript H is the conjugate-transpose operator.

If we take microphone 1 as the reference, we can define the input signal-to-noise ratio (SNR) with respect to this reference as

$$i\text{SNR}(\omega) = \frac{\phi_X(\omega)}{\phi_{V_1}(\omega)}, \quad (7)$$

where $\phi_X(\omega) = E[|X(\omega)|^2]$ and $\phi_{V_1}(\omega) = E[|V_1(\omega)|^2]$ are the variances of $X(\omega)$ and $V_1(\omega)$, respectively, with $E[\cdot]$ denoting mathematical expectation.

The output SNR is obtained from the variance of $Z(\omega)$:

$$\begin{aligned} o\text{SNR}[\mathbf{h}(\omega)] &= \phi_X(\omega) \frac{|\mathbf{h}^H(\omega)\mathbf{d}(\omega, 0)|^2}{\mathbf{h}^H(\omega)\Phi_{\mathbf{v}}(\omega)\mathbf{h}(\omega)} \\ &= \frac{\phi_X(\omega)}{\phi_{V_1}(\omega)} \times \frac{|\mathbf{h}^H(\omega)\mathbf{d}(\omega, 0)|^2}{\mathbf{h}^H(\omega)\Gamma_{\mathbf{v}}(\omega)\mathbf{h}(\omega)}, \end{aligned} \quad (8)$$

where $\Phi_{\mathbf{v}}(\omega) = E[\mathbf{v}(\omega)\mathbf{v}^H(\omega)]$ and $\Gamma_{\mathbf{v}}(\omega) = \frac{\Phi_{\mathbf{v}}(\omega)}{\phi_{V_1}(\omega)}$ are the correlation and pseudo-coherence matrices of $\mathbf{v}(\omega)$, respectively.

The definition of the gain in SNR is easily derived from the previous definitions, i.e.,

$$\mathcal{G}[\mathbf{h}(\omega)] = \frac{o\text{SNR}[\mathbf{h}(\omega)]}{i\text{SNR}(\omega)} = \frac{|\mathbf{h}^H(\omega)\mathbf{d}(\omega, 0)|^2}{\mathbf{h}^H(\omega)\Gamma_{\mathbf{v}}(\omega)\mathbf{h}(\omega)}. \quad (9)$$

We are interested in two types of noise.

- The temporally and spatially white noise with the same variance at all microphones.² In this case, $\Gamma_{\mathbf{v}}(\omega) = \mathbf{I}_M$, where \mathbf{I}_M is the $M \times M$ identity matrix. Therefore, the white noise gain (WNG) is

$$\mathcal{G}_{\text{wn}}[\mathbf{h}(\omega)] = \frac{|\mathbf{h}^H(\omega)\mathbf{d}(\omega, 0)|^2}{\mathbf{h}^H(\omega)\mathbf{h}(\omega)}. \quad (10)$$

The delay-and-sum (DS) beamformer:

² This noise models the sensor noise.

$$\mathbf{h}_{\text{DS}}(\omega) = \frac{\mathbf{d}(\omega, 0)}{M}, \quad (11)$$

leads to the maximum possible WNG given by

$$\mathcal{G}_{\text{wn,max}}(\omega) = M. \quad (12)$$

We will see, actually, how the white noise is amplified, especially at low frequencies, with DMAs.

- The diffuse noise,³ where

$$[\Gamma_{\mathbf{v}}(\omega)]_{ij} = [\Gamma_{\text{dn}}(\omega)]_{ij} = \frac{\sin[\omega(j-i)\tau_0]}{\omega(j-i)\tau_0} = \text{sinc}[\omega(j-i)\tau_0]. \quad (13)$$

In this scenario, the gain in SNR, i.e.,

$$\mathcal{G}_{\text{dn}}[\mathbf{h}(\omega)] = \frac{|\mathbf{h}^H(\omega)\mathbf{d}(\omega, 0)|^2}{\mathbf{h}^H(\omega)\Gamma_{\text{dn}}(\omega)\mathbf{h}(\omega)} \quad (14)$$

is called the directivity factor (DF) and the directivity index is simply defined as [3,7]

$$\mathcal{D}[\mathbf{h}(\omega)] = 10\log_{10}\mathcal{G}_{\text{dn}}[\mathbf{h}(\omega)]. \quad (15)$$

It can be shown that the maximum possible DF is [17]

$$\mathcal{G}_{\text{dn,max}}(\omega) = M^2. \quad (16)$$

This gain can be achieved but at the expense of white noise amplification, especially at low frequencies.

These definitions of the SNRs and gains, which are extremely useful for the evaluation of any types of DMAs, conclude this section.

3. Beampatterns

Each beamformer has a pattern of directional sensitivity, i.e., it has different sensitivities from sounds arriving from different directions. The beampattern or directivity pattern describes the sensitivity of the beamformer to a plane wave (source signal) impinging on the array from the direction θ . For a uniform linear array, it is mathematically defined as

$$\mathcal{B}_M[\mathbf{h}(\omega), \theta] = \mathbf{d}^H(\omega, \theta)\mathbf{h}(\omega) = \sum_{m=1}^M H_m(\omega) e^{j(m-1)\omega\tau_0 \cos\theta}. \quad (17)$$

The frequency-independent beampattern of an N th-order DMA is well known. It is given by [6,7]

$$\mathcal{B}_{\text{D},N}(\theta) = \sum_{n=0}^N a_n \cos^n \theta, \quad (18)$$

where a_n , $n = 0, 1, \dots, N$ are real coefficients. The different values of these coefficients determine the different directivity patterns of the N th-order DMA. There are other ways to express (18) as suggested in [15].

We define the N th-order frequency-independent Chebyshev pattern as

$$\mathcal{B}_{\text{C},N}(\theta) = \sum_{n=0}^N b_n T_n(\cos\theta), \quad (19)$$

where b_n , $n = 0, 1, \dots, N$ are real coefficients and

$$T_n(\cos\theta) = \cos(n\theta), \quad \theta \in [0, \pi], \quad n = 0, 1, \dots, N \quad (20)$$

are Chebyshev polynomials of the first kind [18,19], which have the recurrence relation:

$$T_{n+1}(\cos\theta) = 2\cos\theta \times T_n(\cos\theta) - T_{n-1}(\cos\theta), \quad (21)$$

with

$$T_0(\cos\theta) = 1, \quad T_1(\cos\theta) = \cos\theta.$$

The two patterns $\mathcal{B}_{\text{D},N}(\theta)$ and $\mathcal{B}_{\text{C},N}(\theta)$ are very much related and any DMA pattern can be designed with $\mathcal{B}_{\text{C},N}(\theta)$. Indeed, we know from the usual trigonometric identities that

$$\cos^n \theta = \sum_i c(n, i) \cos[(n-2i)\theta], \quad (22)$$

where $c(n, i)$ are some binomial coefficients. Substituting (22) into (18), we deduce that any DMA pattern can be written as a Chebyshev pattern, $\mathcal{B}_{\text{C},N}(\theta)$. Conversely, $\cos(n\theta)$ can be expressed as a sum of powers of $\cos\theta$ thanks to the recurrence relation (21). Consequently, any Chebyshev pattern can be written as a DMA pattern. We can then conclude that $\mathcal{B}_{\text{D},N}(\theta)$ and $\mathcal{B}_{\text{C},N}(\theta)$ are strictly equivalent. In this study, $\mathcal{B}_{\text{C},N}(\theta)$ is preferred as it will become clear soon.

The relations between the coefficients b_n , $n = 0, 1, \dots, N$ of $\mathcal{B}_{\text{C},N}(\theta)$ and the coefficients a_n , $n = 0, 1, \dots, N$ of $\mathcal{B}_{\text{D},N}(\theta)$ for the first three orders are as follows:

- $N = 1$: $b_0 = a_0, b_1 = a_1$;
- $N = 2$: $b_0 = a_0 + \frac{a_2}{2}, b_1 = a_1, b_2 = \frac{a_2}{2}$; and
- $N = 3$: $b_0 = a_0 + \frac{a_2}{2}, b_1 = a_1 + \frac{3a_3}{4}, b_2 = \frac{a_2}{2}, b_3 = \frac{a_3}{4}$.

Now, one may ask how are (17) and (19) related? Let us denote by

$$\varpi_m = (m-1)\omega\tau_0. \quad (23)$$

The Jacobi–Anger expansion [20,21], which represents an expansion of plane waves into a series of cylindrical waves, is given by

$$e^{j\varpi_m \cos\theta} = J_0(\varpi_m) + 2\sum_{n=1}^{\infty} j^n J_n(\varpi_m) \cos(n\theta) = \sum_{n=0}^{\infty} j_n J_n(\varpi_m) \cos(n\theta), \quad (24)$$

where

$$j_n = \begin{cases} 1, & n = 0 \\ 2j^n, & n = 1, 2, \dots, N \end{cases} \quad (25)$$

and

$$J_n(\varpi_m) = \left(\frac{1}{2}\varpi_m\right)^n \sum_{k=0}^{\infty} \frac{(-\frac{1}{4}\varpi_m^2)^k}{k!\Gamma(n+k+1)} \quad (26)$$

is the n th-order Bessel function of the first kind [18]. In Appendix A, we prove that the Jacobi–Anger expansion is the optimal approximation of $e^{j\varpi_m \cos\theta}$ in the mean-squared error (MSE) sense. Using (24) in the general definition of the beampattern, we obtain

$$\begin{aligned} \mathcal{B}_M[\mathbf{h}(\omega), \theta] &= \sum_{m=1}^M H_m(\omega) e^{j\varpi_m \cos\theta} = \sum_{m=1}^M H_m(\omega) \sum_{n=0}^{\infty} j_n J_n(\varpi_m) \cos(n\theta) \\ &= \sum_{n=0}^{\infty} \cos(n\theta) \left[\sum_{m=1}^M j_n J_n(\varpi_m) H_m(\omega) \right]. \end{aligned} \quad (27)$$

If we limit the expansion to the order N , $\mathcal{B}_M[\mathbf{h}(\omega), \theta]$ can be approximated by

$$\mathcal{B}_{M,N}[\mathbf{h}(\omega), \theta] = \sum_{n=0}^N \cos(n\theta) \left[\sum_{m=1}^M j_n J_n(\varpi_m) H_m(\omega) \right]. \quad (28)$$

For $m = 1$, $\varpi_1 = 0$, so that $J_0(\varpi_1) = 1$ and $J_n(\varpi_1) = 0$, $n = 1, 2, \dots, N$. We will see how to use (28) in order to design both traditional and robust DMAs of different orders.

³ This situation corresponds to the spherically isotropic noise field.

4. Robust first-order DMAs

Let us assume that δ is very small (implying that ϖ_m is also very small), so that $\mathcal{B}_{M,N}[\mathbf{h}(\omega), \theta]$ with $N = 1$ approximates well $\mathcal{B}_M[\mathbf{h}(\omega), \theta]$. Then, we have

$$\mathcal{B}_{M,1}[\mathbf{h}(\omega), \theta] = \sum_{m=1}^M H_m(\omega) [J_0(\varpi_m) + 2J_1(\varpi_m) \cos \theta]. \quad (29)$$

We study two cases: $M = 2$ and $M > 2$. The latter is considered as the robust approach, while the former is the traditional one, which is not robust.

For $M = 2$, we can express (29) as

$$\mathcal{B}_{2,1}[\mathbf{h}(\omega), \theta] = H_1(\omega) + J_0(\varpi_2)H_2(\omega) + 2J_1(\varpi_2)H_2(\omega) \cos \theta. \quad (30)$$

Now, we wish to find $H_1(\omega)$ and $H_2(\omega)$ in such a way that $\mathcal{B}_{2,1}[\mathbf{h}(\omega), \theta]$ is a first-order frequency-invariant Chebyshev pattern, i.e.,

$$\mathcal{B}_{2,1}[\mathbf{h}(\omega), \theta] = b_0 + b_1 \cos \theta = \mathcal{B}_{C,1}(\theta). \quad (31)$$

Identifying the previous expression with (30), we easily find that

$$H_2(\omega) = \frac{b_1}{2J_1(\varpi_2)} \quad (32)$$

and

$$H_1(\omega) = -J_0(\varpi_2)H_2(\omega) + b_0. \quad (33)$$

Therefore, with this approach, we can design any first-order DMA. In some interval of very high frequencies, $J_1(\varpi_2)$ may have some zeros. Therefore, if $J_1(\varpi_2) = 0$ for some very few high frequencies, the best thing to do is to not process the microphone signals at those frequencies. This, however, never happens below 8 kHz.

The case $M > 2$ is more interesting. We still want to find the coefficients $H_m(\omega)$, $m = 1, 2, \dots, M$ in such a way that $\mathcal{B}_{M,1}[\mathbf{h}(\omega), \theta] = \mathcal{B}_{C,1}(\theta)$. It is not hard to get

$$[J_1(\varpi_2) \quad J_1(\varpi_3) \quad \dots \quad J_1(\varpi_M)] \begin{bmatrix} H_2(\omega) \\ H_3(\omega) \\ \vdots \\ H_M(\omega) \end{bmatrix} = \frac{b_1}{2} \quad (34)$$

and

$$H_1(\omega) + \sum_{i=2}^M J_0(\varpi_i)H_i(\omega) = b_0. \quad (35)$$

Taking the minimum-norm solution of (34), it is clear that the filter coefficients are as follows:

$$H_i(\omega) = \frac{J_1(\varpi_i)b_1}{2J \sum_{m=2}^M J_1^2(\varpi_m)}, \quad i = 2, 3, \dots, M \quad (36)$$

and

$$H_1(\omega) = -\sum_{i=2}^M J_0(\varpi_i)H_i(\omega) + b_0. \quad (37)$$

The beamformer, $\mathbf{h}(\omega)$, whose components are given in (37) and (36), is the minimum-norm filter for robust first-order DMAs. In Appendix B, we demonstrate that the white noise gain of the proposed first-order DMA is generally an increasing function of M , the number of microphones.

5. Robust second-order DMAs

We follow the same methodology as in the previous section but, this time, we assume that $\mathcal{B}_{M,N}[\mathbf{h}(\omega), \theta]$ with $N = 2$ approximates well $\mathcal{B}_M[\mathbf{h}(\omega), \theta]$. Therefore,

$$\mathcal{B}_{M,2}[\mathbf{h}(\omega), \theta] = \sum_{m=1}^M H_m(\omega) [J_0(\varpi_m) + 2J_1(\varpi_m) \cos \theta - 2J_2(\varpi_m) \cos(2\theta)]. \quad (38)$$

We are ready to study the non-robust ($M = 3$) and robust ($M > 3$) cases.

For $M = 3$, we can rewrite (38) as

$$\begin{aligned} \mathcal{B}_{3,2}[\mathbf{h}(\omega), \theta] &= H_1(\omega) + J_0(\varpi_2)H_2(\omega) + J_0(\varpi_3)H_3(\omega) \\ &\quad + 2J_1(\varpi_2)H_2(\omega) \cos \theta + 2J_1(\varpi_3)H_3(\omega) \cos \theta \\ &\quad - 2J_2(\varpi_2)H_2(\omega) \cos(2\theta) - 2J_2(\varpi_3)H_3(\omega) \cos(2\theta). \end{aligned} \quad (39)$$

Our aim is to find $H_1(\omega)$, $H_2(\omega)$, and $H_3(\omega)$ in such a way that $\mathcal{B}_{3,2}[\mathbf{h}(\omega), \theta]$ is a second-order frequency-invariant Chebyshev pattern, i.e.,

$$\mathcal{B}_{3,2}[\mathbf{h}(\omega), \theta] = b_0 + b_1 \cos \theta + b_2 \cos(2\theta) = \mathcal{B}_{C,2}(\theta). \quad (40)$$

By simple identification, we find that the solution is

$$\begin{bmatrix} H_2(\omega) \\ H_3(\omega) \end{bmatrix} = \begin{bmatrix} J_1(\varpi_2) & J_1(\varpi_3) \\ J_2(\varpi_2) & J_2(\varpi_3) \end{bmatrix}^{-1} \begin{bmatrix} \frac{b_1}{2} \\ -\frac{b_2}{2} \end{bmatrix} \quad (41)$$

and

$$H_1(\omega) = -J_0(\varpi_2)H_2(\omega) - J_0(\varpi_3)H_3(\omega) + b_0. \quad (42)$$

We see that we can design any second-order DMA.

For $M > 3$, we still want to find the coefficients $H_m(\omega)$, $m = 1, 2, \dots, M$ in such a way that $\mathcal{B}_{M,2}[\mathbf{h}(\omega), \theta] = \mathcal{B}_{C,2}(\theta)$. It is not hard to find that the solution is

$$\begin{bmatrix} H_2(\omega) \\ H_3(\omega) \\ \vdots \\ H_M(\omega) \end{bmatrix} = \mathbf{Y}_2^T(\omega) [\mathbf{Y}_2(\omega) \mathbf{Y}_2^T(\omega)]^{-1} \begin{bmatrix} \frac{b_1}{2} \\ -\frac{b_2}{2} \end{bmatrix} \quad (43)$$

and

$$H_1(\omega) = -\sum_{i=2}^M J_0(\varpi_i)H_i(\omega) + b_0. \quad (44)$$

where

$$\mathbf{Y}_2(\omega) = \begin{bmatrix} J_1(\varpi_2) & J_1(\varpi_3) & \dots & J_1(\varpi_M) \\ J_2(\varpi_2) & J_2(\varpi_3) & \dots & J_2(\varpi_M) \end{bmatrix} \quad (45)$$

is a $2 \times (M - 1)$ matrix.

6. Robust third-order DMAs

Following the same ideas as before, it is easy to see that the coefficients of the filter for the design of robust third-order DMAs are given by

$$\begin{bmatrix} H_2(\omega) \\ H_3(\omega) \\ \vdots \\ H_M(\omega) \end{bmatrix} = \mathbf{Y}_3^T(\omega) [\mathbf{Y}_3(\omega) \mathbf{Y}_3^T(\omega)]^{-1} \begin{bmatrix} \frac{b_1}{2} \\ -\frac{b_2}{2} \\ -\frac{b_3}{2} \end{bmatrix} \quad (46)$$

and

$$H_1(\omega) = -\sum_{i=2}^M J_0(\varpi_i)H_i(\omega) + b_0. \tag{47}$$

where

$$\Upsilon_3(\omega) = \begin{bmatrix} J_1(\varpi_2) & J_1(\varpi_3) & \cdots & J_1(\varpi_M) \\ J_2(\varpi_2) & J_2(\varpi_3) & \cdots & J_2(\varpi_M) \\ J_3(\varpi_2) & J_3(\varpi_3) & \cdots & J_3(\varpi_M) \end{bmatrix} \tag{48}$$

is a $3 \times (M - 1)$ matrix. Now, the number of microphones must be at least equal to four.

The generalization of this approach to any order is straightforward. However, in practice, we almost never go beyond the third order because of the white noise amplification problem.

7. Simulations

In this section, we evaluate the performance of the proposed DMAs through simulations. We always take the interelement spacing $\delta = 1.5$ cm and assume that the desired signal is at the endfire direction. In the rest, we would like to design DMAs that have the following first-, second-, and third-order frequency-independent Chebyshev patterns:

$$\mathcal{B}_{C,1}(\theta) = 0.414 + 0.586 \cos \theta, \tag{49}$$

$$\mathcal{B}_{C,2}(\theta) = 0.3095 + 0.484 \cos \theta + 0.2065 \cos(2\theta), \tag{50}$$

$$\mathcal{B}_{C,3}(\theta) = 0.2595 + 0.4315 \cos \theta + 0.2375 \cos(2\theta) + 0.0715 \cos(3\theta). \tag{51}$$

They are equivalent to the first-, second-, and third-order supercardioid patterns [16]:

$$\mathcal{B}_{D,1}(\theta) = 0.414 + 0.586 \cos \theta, \tag{52}$$

$$\mathcal{B}_{D,2}(\theta) = 0.103 + 0.484 \cos \theta + 0.413 \cos^2 \theta, \tag{53}$$

$$\mathcal{B}_{D,3}(\theta) = 0.022 + 0.217 \cos \theta + 0.475 \cos^2 \theta + 0.286 \cos^3 \theta. \tag{54}$$

These supercardioid patterns are illustrated in Figs. 2–4.

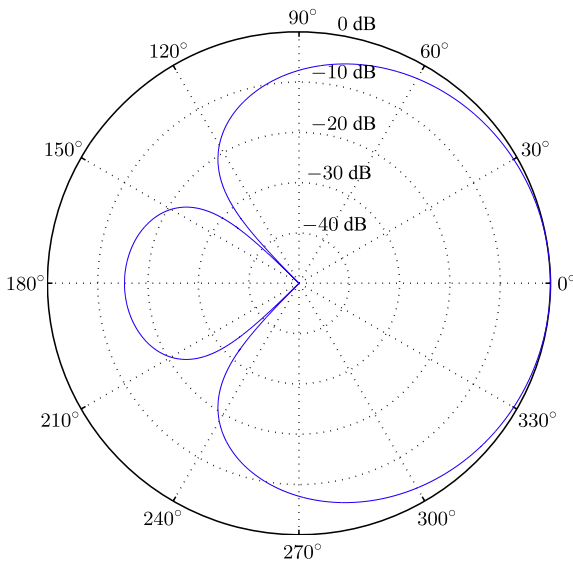


Fig. 2. First-order supercardioid pattern.

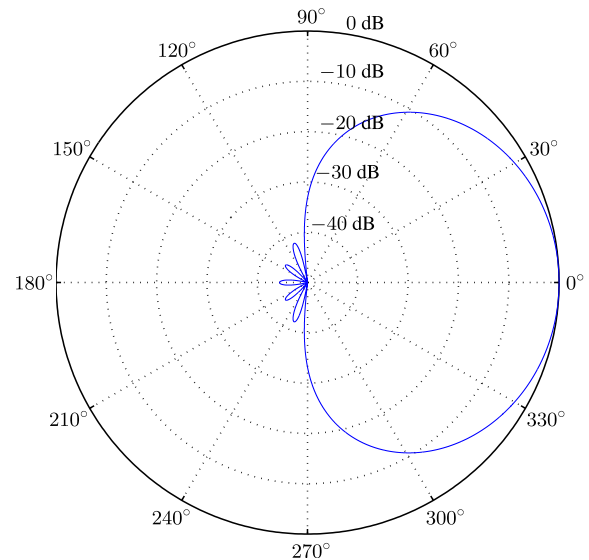


Fig. 4. Third-order supercardioid pattern.

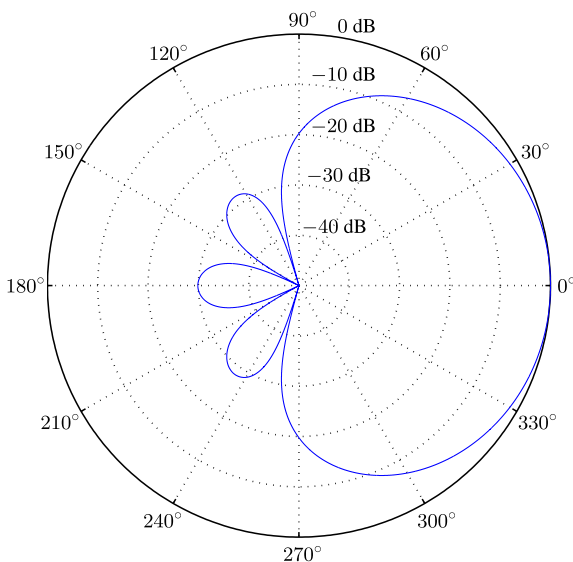


Fig. 3. Second-order supercardioid pattern.

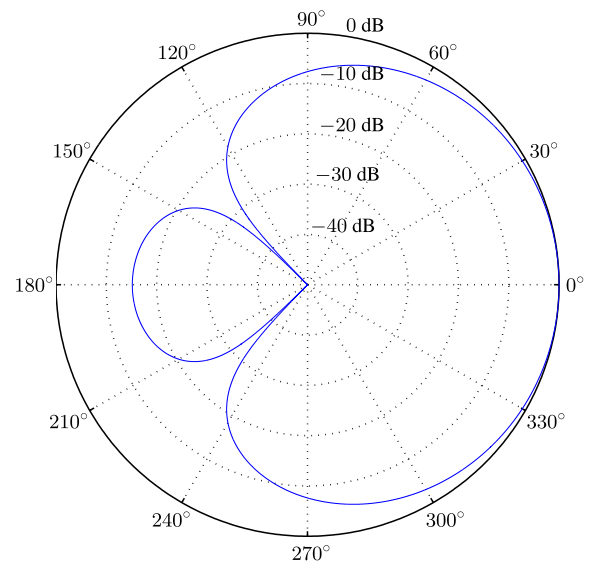


Fig. 5. Pattern of the traditional first-order DMA designed with the Jacobi-Anger expansion. $M = 2$, $\delta = 1.5$ cm, and $f = 1$ kHz.

7.1. First-order DMAs

In the first set of simulations, we study the performance of the first-order DMAs. First, we deal with the traditional first-order DMA by setting $M = 2$. The corresponding pattern and SNR gains are presented in Figs. 5 and 6. Comparing Figs. 5 and 2, we can see that the pattern of the traditional first-order DMA is very close to the first-order supercardioid pattern, where the desired signal from the endfire direction is perfectly preserved while the signals from other directions are attenuated, especially the signals from the angles 135° and 225° . From the SNR gains in Fig. 6, we can see that the DF is constant and its value is around 5 dB while the WNG is negative for most frequencies, indicating that the traditional first-order DMA has the problem of white noise amplification. Then, by using more microphones (i.e., $M = 4$ and $M = 6$) and minimum-norm filters, we derive robust first-order DMAs. Their performance are plotted in Figs. 7–10. It is shown that the

patterns of the robust first-order DMAs are similar to the pattern of the traditional first-order DMA. Comparing the results in Figs. 6, 8, and 10, we can observe that the WNG improves significantly as M increases from 2 to 6. This observation confirms that robust first-order DMAs are more robust against white noise amplification than the traditional first-order DMA.

For comparison, we also derived first-order DMAs with the MacLaurin's series and the frequency-independent supercardioid pattern $\mathcal{B}_{D,1}(\theta)$ [6,8]. The results are presented in Figs. 11–16. Comparing them with the previous ones in Figs. 5–10, we can see that the patterns of the DMAs based on the Jacobi–Anger expansion are closer to the supercardioid patterns than the patterns of the DMAs based on the MacLaurin's series. To better illustrate this superiority, we put the patterns of the DMAs based on the Jacobi–Anger

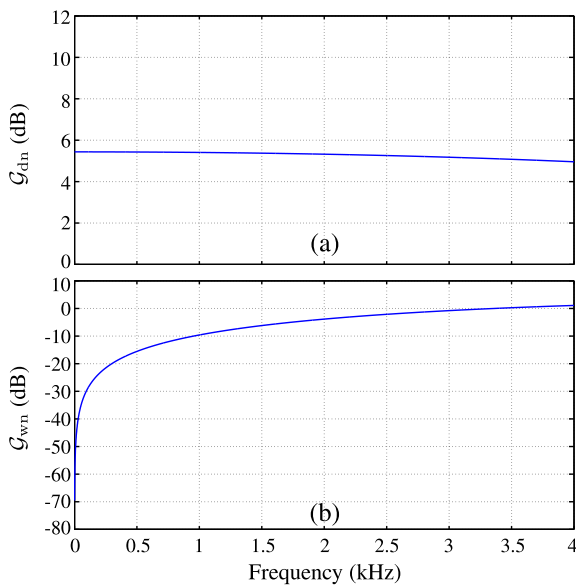


Fig. 6. SNR gains of the traditional first-order DMA designed with the Jacobi–Anger expansion: (a) DF and (b) WNG. $M = 2$ and $\delta = 1.5$ cm.

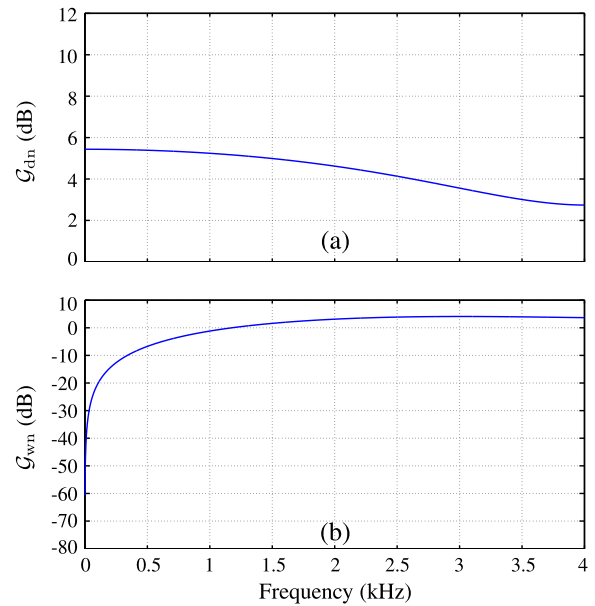


Fig. 8. SNR gains of the robust first-order DMA designed with the Jacobi–Anger expansion: (a) DF and (b) WNG. $M = 4$ and $\delta = 1.5$ cm.

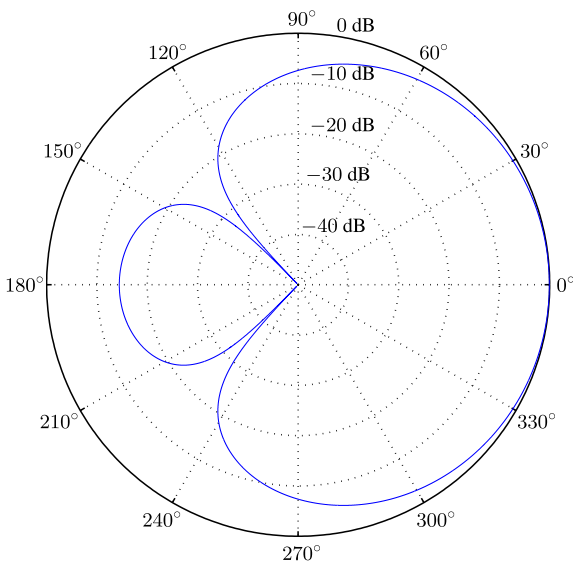


Fig. 7. Pattern of the robust first-order DMA designed with the Jacobi–Anger expansion. $M = 4$, $\delta = 1.5$ cm, and $f = 1$ kHz.

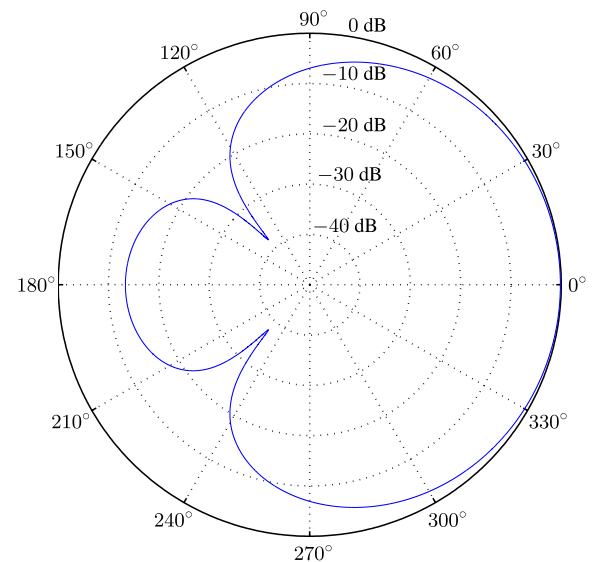


Fig. 9. Pattern of the robust first-order DMA designed with the Jacobi–Anger expansion. $M = 6$, $\delta = 1.5$ cm, and $f = 1$ kHz.

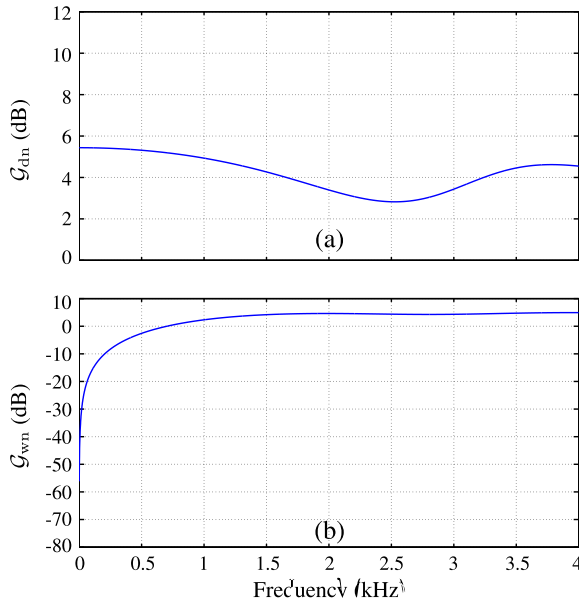


Fig. 10. SNR gains of the robust first-order DMA designed with the Jacobi–Anger expansion: (a) DF and (b) WNG. $M = 6$ and $\delta = 1.5$ cm.

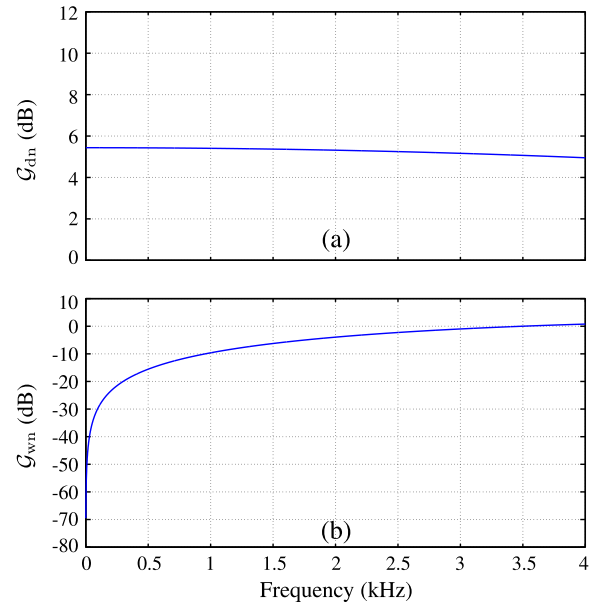


Fig. 12. SNR gains of the traditional first-order DMA designed with the Maclaurin's series: (a) DF and (b) WNG. $M = 2$ and $\delta = 1.5$ cm.

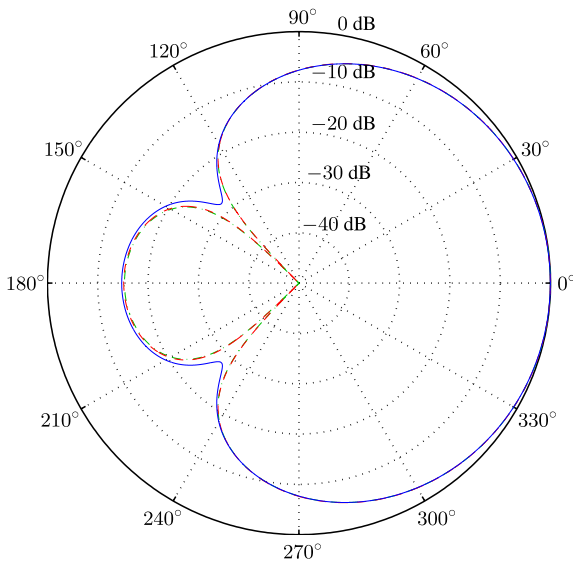


Fig. 11. Pattern of the traditional first-order DMA designed with the Maclaurin's series (blue solid), pattern of the traditional first-order DMA designed with the Jacobi–Anger expansion (red dashed), and desired first-order supercardioid pattern (green dashdot). $M = 2$, $\delta = 1.5$ cm, and $f = 1$ kHz.

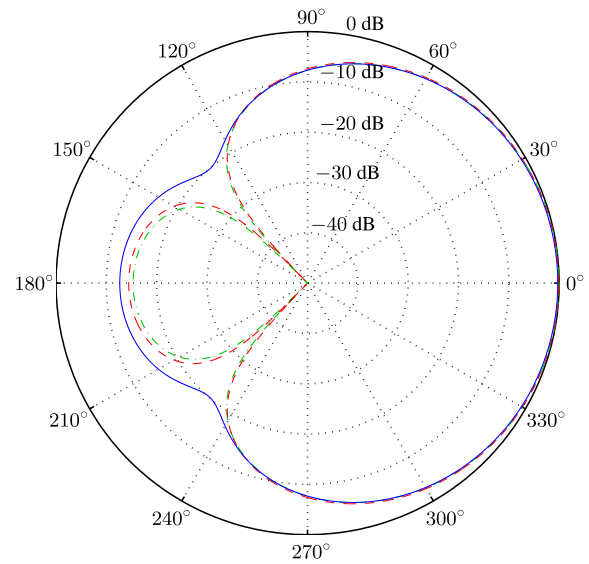


Fig. 13. Pattern of the robust first-order DMA designed with the Maclaurin's series (blue solid), pattern of the robust first-order DMA designed with the Jacobi–Anger expansion (red dashed), and desired first-order supercardioid pattern (green dashdot). $M = 4$, $\delta = 1.5$ cm, and $f = 1$ kHz.

expansion and the desired supercardioid pattern into Figs. 11, 13, and 15. In addition, the DMAs designed with the Jacobi–Anger expansion are superior in terms of DF and WNG as shown in Figs. 10 and 16 (for $M = 6$). This superiority is more obvious when $M = 6$ and $f > 2$ kHz. This result may be explained as follows. When M is large and the frequency is high, the exponent of $e^{j(m-1)\omega r_0 \cos \theta}$ for $m > 1$ may be far away from zero. In this case, the Maclaurin's series approximation is very inaccurate, whereas the approximation based on the Jacobi–Anger expansion can still perform well. Therefore, we can claim that the Jacobi–Anger expansion is preferred in the design of DMAs.

7.2. Second-order DMAs

The performance of the second-order DMAs is investigated in this second set of simulations. We first plot, in Figs. 17 and 18, the performance of the traditional second-order DMA (with $M = 3$). We can see that its pattern is similar to the second-order supercardioid pattern in Fig. 3, in that the desired signal from the endfire direction is well preserved while the signals from other directions are well attenuated. We can also see that the traditional second-order DMA gives a constant DF a bit higher than 8 dB, but there is white noise amplification. Comparing the WNGs in Figs. 18

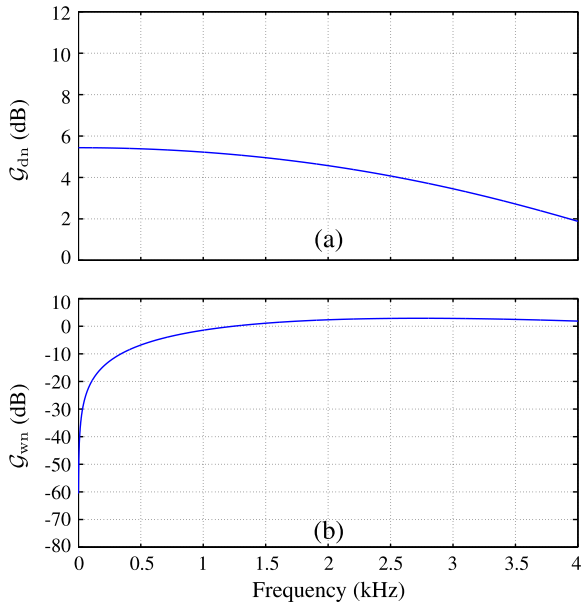


Fig. 14. SNR gains of the robust first-order DMA designed with the MacLaurin's series: (a) DF and (b) WNG. $M = 4$ and $\delta = 1.5$ cm.

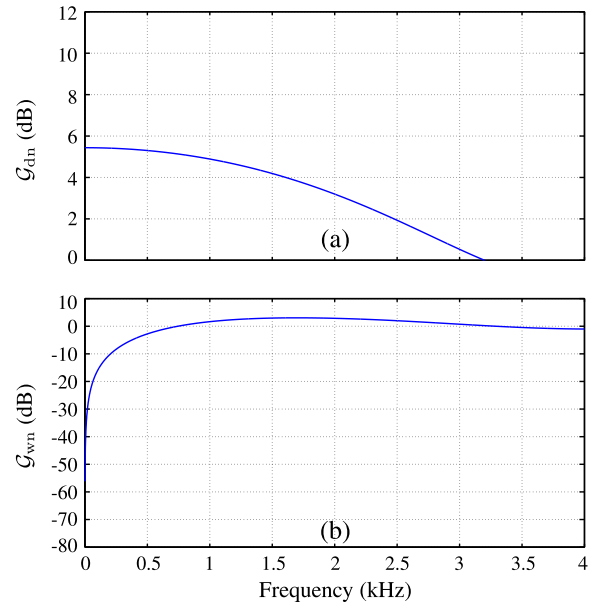


Fig. 16. SNR gains of the robust first-order DMA designed with the MacLaurin's series: (a) DF and (b) WNG. $M = 6$ and $\delta = 1.5$ cm.

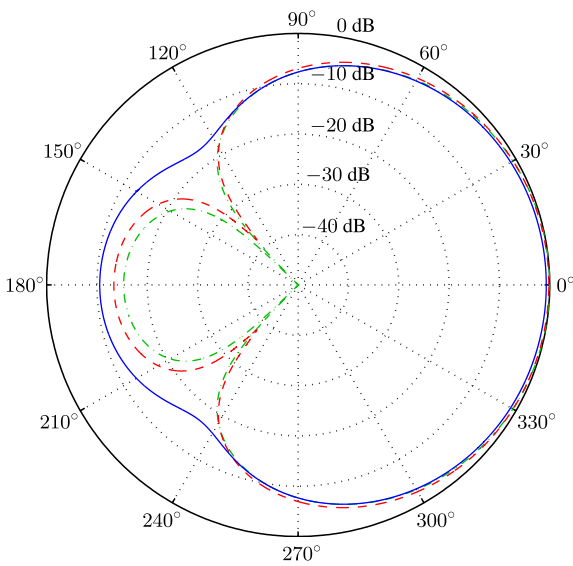


Fig. 15. Pattern of the robust first-order DMA designed with the MacLaurin's series (blue solid), pattern of the robust first-order DMA designed with the Jacobi-Anger expansion (red dashed), and desired first-order supercardioid pattern (green dashdot). $M = 6$, $\delta = 1.5$ cm, and $f = 1$ kHz.

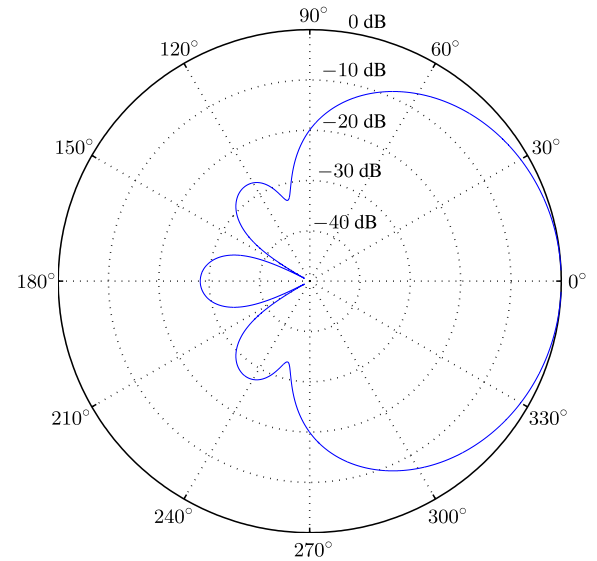


Fig. 17. Pattern of the traditional second-order DMA designed with the Jacobi-Anger expansion. $M = 3$, $\delta = 1.5$ cm, and $f = 1$ kHz.

and 6, we can easily observe that the problem of white noise amplification, especially at low frequencies, becomes more serious as the order of the traditional DMA increases from 1 to 2. Then, we derive robust second-order DMAs by setting the number of microphones to $M = 5$ and $M = 8$, respectively. The corresponding patterns and SNR gains are plotted in Figs. 19–22. It is seen that increasing the value of M improves the WNG considerably while the pattern and the DF are not that much affected. For example, at 500 Hz, for $M = 3$, the WNG is equal to -35 dB while it is equal to -10 dB for $M = 8$; this represents an improvement of 25 dB. The DF, on the other hand, is identical for both values of M at that frequency.

7.3. Third-order DMAs

Finally, we evaluate the performance of the third-order DMA by setting the number of microphones to $M = 4$, $M = 7$, and $M = 10$, respectively. As shown in Figs. 23–28, the number of microphones greatly influences the performance of the third-order DMA in a similar way as it does to the performance of the first- and second-order DMAs, i.e., the WNG is significantly improved while the pattern and the DF do not change much as M increases. Therefore, with a larger number of microphones, the proposed third-order DMA can be more robust against white noise amplification.

8. Conclusions

In this paper, we have focused on a new way to design DMAs. Based on the Jacobi-Anger expansion and the frequency-

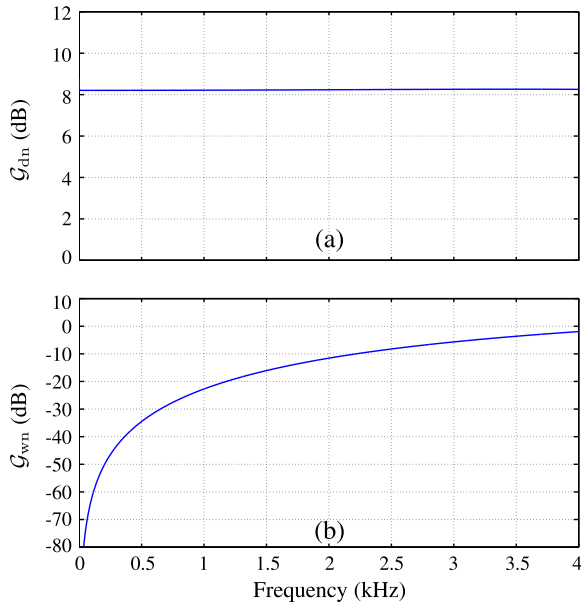


Fig. 18. SNR gains of the traditional second-order DMA designed with the Jacobi–Anger expansion: (a) DF and (b) WNG. $M = 3$ and $\delta = 1.5$ cm.

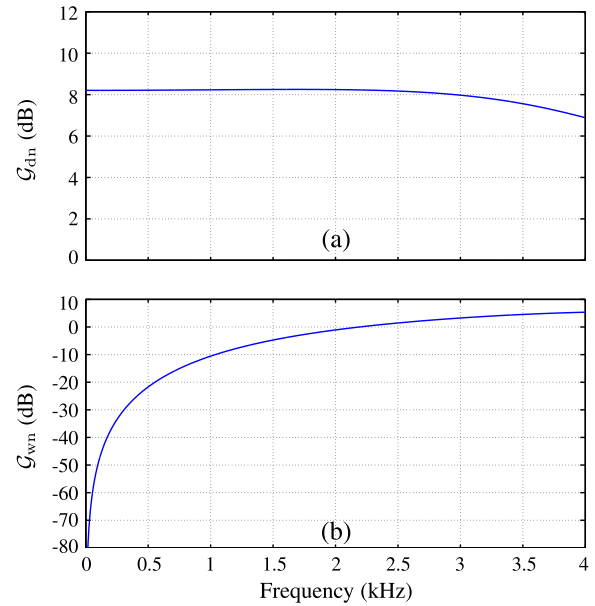


Fig. 20. SNR gains of the robust second-order DMA designed with the Jacobi–Anger expansion: (a) DF and (b) WNG. $M = 5$ and $\delta = 1.5$ cm.

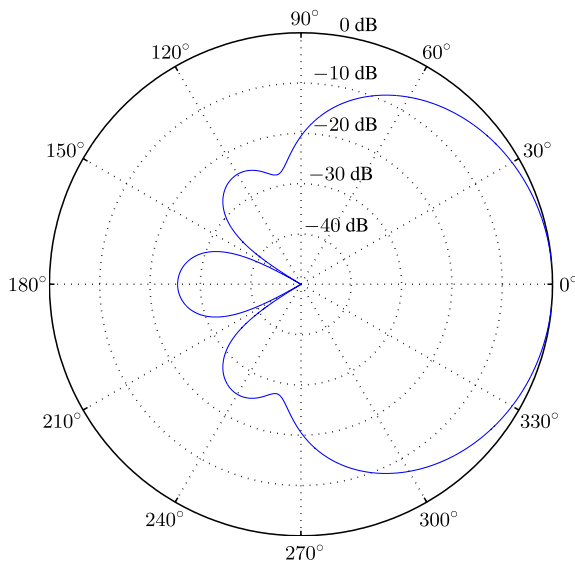


Fig. 19. Pattern of the robust second-order DMA designed with the Jacobi–Anger expansion. $M = 5$, $\delta = 1.5$ cm, and $f = 1$ kHz.

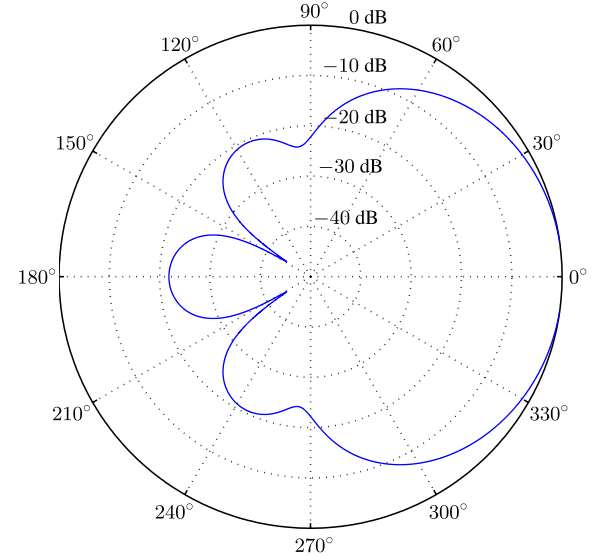


Fig. 21. Pattern of the robust second-order DMA designed with the Jacobi–Anger expansion. $M = 8$, $\delta = 1.5$ cm, and $f = 1$ kHz.

independent Chebyshev patterns, we derived the traditional (non-robust) first-, second-, and third-order DMAs. Simulation results showed that the traditional DMAs with this approach achieve large SNR gains in diffuse noise, but at the expense of white noise amplification, like in all conventional DMAs. We also derived robust DMAs by using more microphones and minimum-norm filters. These DMAs were verified, through many simulations, to have significantly higher WNGs than the traditional DMAs. In addition, we also compared, by way of simulations, this new method to the recently proposed one based on the MacLaurin's series approximation. All our results show that the new one has much better performance; this advantage becomes more noticeable when the number of microphones is large and the frequency is high.

Appendix A

In this section, we prove that the Jacobi–Anger expansion is the optimal approximation of $e^{j\sigma_m \cos \theta}$ in the mean-squared error (MSE) sense. But before presenting the proof, we define two useful Bessel functions.

The Bessel function of the first kind is [18]

$$J_n(z) = \left(\frac{1}{2}z\right)^n \sum_{k=0}^{\infty} \frac{(-\frac{1}{4}z^2)^k}{k! \Gamma(n+k+1)}, \quad (55)$$

where n and z are the order and variable, respectively. The modified Bessel function of the first kind is [18]

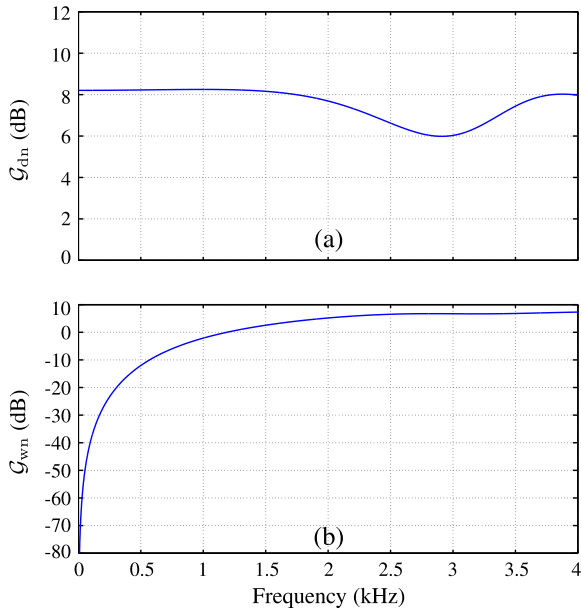


Fig. 22. SNR gains of the robust second-order DMA designed with the Jacobi–Anger expansion: (a) DF and (b) WNG. $M = 8$ and $\delta = 1.5$ cm.

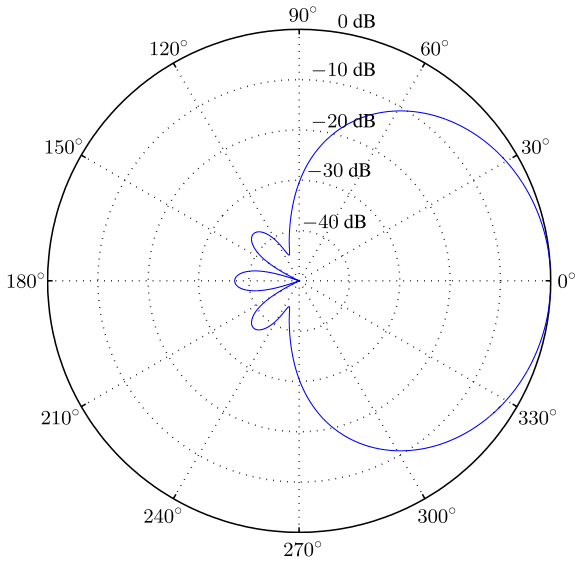


Fig. 23. Pattern of the traditional third-order DMA designed with the Jacobi–Anger expansion. $M = 4$, $\delta = 1.5$ cm, and $f = 1$ kHz.

$$I_n(z) = \left(\frac{1}{2}z\right)^n \sum_{k=0}^{\infty} \frac{\left(\frac{1}{4}z^2\right)^k}{k! \Gamma(n+k+1)}, \quad (56)$$

and its integral representation is

$$I_n(z) = \frac{1}{\pi} \int_0^{\pi} e^{z \cos \theta} \cos(n\theta) d\theta. \quad (57)$$

It can be checked that

$$I_n(jz) = j^n J_n(z). \quad (58)$$

We recall that the exponential function $e^{j\varpi_m \cos \theta}$ can be approximated by [6,8]

$$e^{j\varpi_m \cos \theta} = \lim_{N \rightarrow \infty} \sum_{n=0}^N a_n \cos^n \theta, \quad (59)$$

where N is the approximation order and $a_n, n = 0, 1, \dots, N$ are complex coefficients. Thanks to the trigonometric identities, the expression in (59) can also be written as

$$e^{j\varpi_m \cos \theta} = \lim_{N \rightarrow \infty} \sum_{n=0}^N c_n \cos(n\theta), \quad (60)$$

where $c_n, n = 0, 1, \dots, N$ are complex coefficients. Here, we use (60) to derive the optimal approximation of $e^{j\varpi_m \cos \theta}$ in the MSE sense.

Based on (60) and assuming that θ is a real random variable, we define the MSE criterion of the N th-order approximation as

$$\text{MSE}(N) = E \left[\left| e^{j\varpi_m \cos \theta} - \sum_{n=0}^N c_n \cos(n\theta) \right|^2 \right]. \quad (61)$$

Our goal is to find the coefficients $c_n, n = 0, 1, \dots, N$ in such a way that $\text{MSE}(N)$ is minimized. Mathematically, this is equivalent to

$$\min_{c_0, c_1, \dots, c_N} \text{MSE}(N) = \min_{c_0, c_1, \dots, c_N} E \left[\left| e^{j\varpi_m \cos \theta} - \sum_{n=0}^N c_n \cos(n\theta) \right|^2 \right]. \quad (62)$$

First, we consider the first-order approximation. By setting $N = 1$ in (61), we have

$$\begin{aligned} \text{MSE}(1) &= E \left[\left| e^{j\varpi_m \cos \theta} - c_0 - c_1 \cos \theta \right|^2 \right] \\ &= E \left[(e^{j\varpi_m \cos \theta} - c_0 - c_1 \cos \theta)(e^{-j\varpi_m \cos \theta} - c_0^* - c_1^* \cos \theta) \right] \end{aligned} \quad (63)$$

To obtain the minimum value of $\text{MSE}(1)$, we compute the gradients of $\text{MSE}(1)$ with respect to $c_n^*, n = 0, 1$, and equate the results to zero, i.e.,

$$\frac{\partial \text{MSE}(1)}{\partial c_0^*} = -E(e^{j\varpi_m \cos \theta}) + c_0 + c_1 E(\cos \theta) = 0 \quad (64)$$

and

$$\frac{\partial \text{MSE}(1)}{\partial c_1^*} = -E(e^{j\varpi_m \cos \theta} \cos \theta) + c_0 E(\cos \theta) + c_1 E(\cos^2 \theta) = 0. \quad (65)$$

Using (55)–(57) and assuming that θ is uniformly distributed in the interval $[0, \pi]$, we can compute the expectations in (64) and (65) as

$$E(\cos \theta) = \frac{1}{\pi} \int_0^{\pi} \cos \theta d\theta = 0, \quad (66)$$

$$E(\cos^2 \theta) = \frac{1}{\pi} \int_0^{\pi} \cos^2 \theta d\theta = \frac{1}{\pi} \int_0^{\pi} \frac{1}{2} [1 + \cos(2\theta)] d\theta = \frac{1}{2}, \quad (67)$$

$$E(e^{j\varpi_m \cos \theta}) = \frac{1}{\pi} \int_0^{\pi} e^{j\varpi_m \cos \theta} d\theta = I_0(j\varpi_m) = J_0(\varpi_m), \quad (68)$$

$$E(e^{j\varpi_m \cos \theta} \cos \theta) = \frac{1}{\pi} \int_0^{\pi} e^{j\varpi_m \cos \theta} \cos \theta d\theta = I_1(j\varpi_m) = jJ_1(\varpi_m). \quad (69)$$

Substituting (66)–(69) into (64) and (65), we obtain

$$c_0 = J_0(\varpi_m), \quad (70)$$

$$c_1 = 2jJ_1(\varpi_m). \quad (71)$$

As a result, the optimal first-order approximation of $e^{j\varpi_m \cos \theta}$ is

$$e^{j\varpi_m \cos \theta} = J_0(\varpi_m) + 2jJ_1(\varpi_m) \cos \theta. \quad (72)$$

Now, we consider the second-order approximation, i.e., $N = 2$. From (61), we have

$$\begin{aligned} \text{MSE}(2) &= E \left[\left| e^{j\varpi_m \cos \theta} - c_0 - c_1 \cos \theta - c_2 \cos(2\theta) \right|^2 \right] \\ &= E \left\{ \left[e^{j\varpi_m \cos \theta} - c_0 - c_1 \cos \theta - c_2 \cos(2\theta) \right] \left[e^{-j\varpi_m \cos \theta} - c_0^* - c_1^* \cos \theta - c_2^* \cos(2\theta) \right] \right\}. \end{aligned} \quad (73)$$

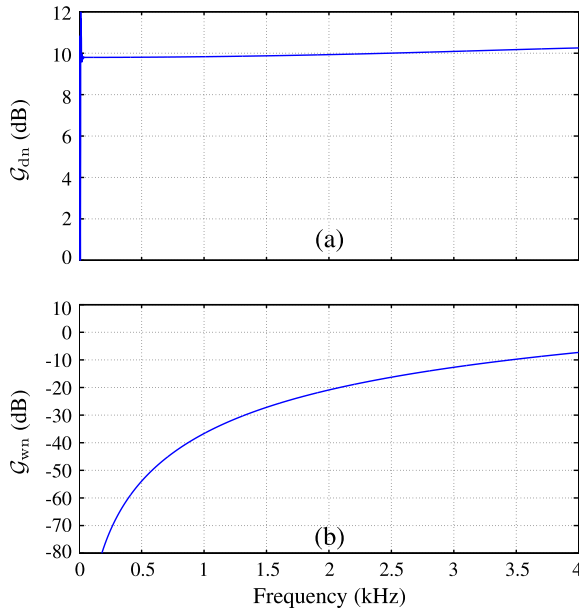


Fig. 24. SNR gains of the traditional third-order DMA designed with the Jacobi-Anger expansion: (a) DF and (b) WNG. $M = 4$ and $\delta = 1.5$ cm.

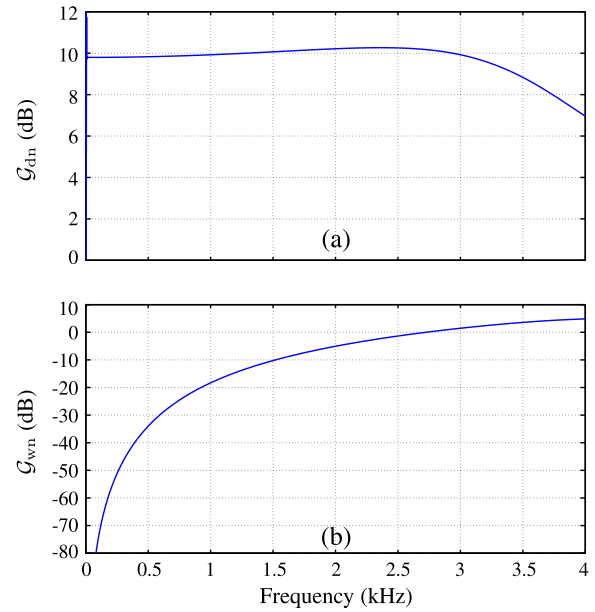


Fig. 26. SNR gains of the robust third-order DMA designed with the Jacobi-Anger expansion: (a) DF and (b) WNG. $M = 7$ and $\delta = 1.5$ cm.

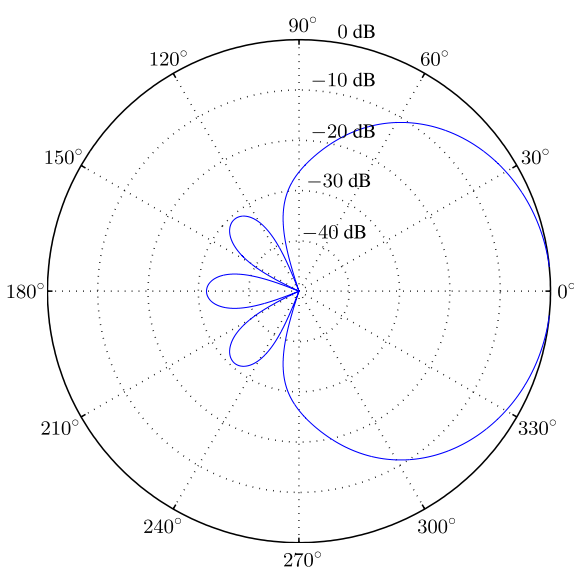


Fig. 25. Pattern of the robust third-order DMA designed with the Jacobi-Anger expansion. $M = 7$, $\delta = 1.5$ cm and $f = 1$ kHz.

By computing the gradients of $MSE(2)$ with respect to c_n^* , $n = 0, 1, 2$ and equating the results to zero, we get

$$\frac{\partial MSE(2)}{\partial c_0^*} = -E(e^{j\varpi_m \cos \theta}) + c_0 + c_1 E(\cos \theta) + c_2 E[\cos(2\theta)] = 0, \quad (74)$$

$$\frac{\partial MSE(2)}{\partial c_1^*} = -E(e^{j\varpi_m \cos \theta} \cos \theta) + c_0 E(\cos \theta) + c_1 E(\cos^2 \theta) + c_2 E[\cos(2\theta) \cos \theta] = 0, \quad (75)$$

$$\frac{\partial MSE(2)}{\partial c_2^*} = -E[e^{j\varpi_m \cos \theta} \cos(2\theta)] + c_0 E[\cos(2\theta)] + c_1 E[\cos \theta \cos(2\theta)] + c_2 E[\cos^2(2\theta)] = 0. \quad (76)$$

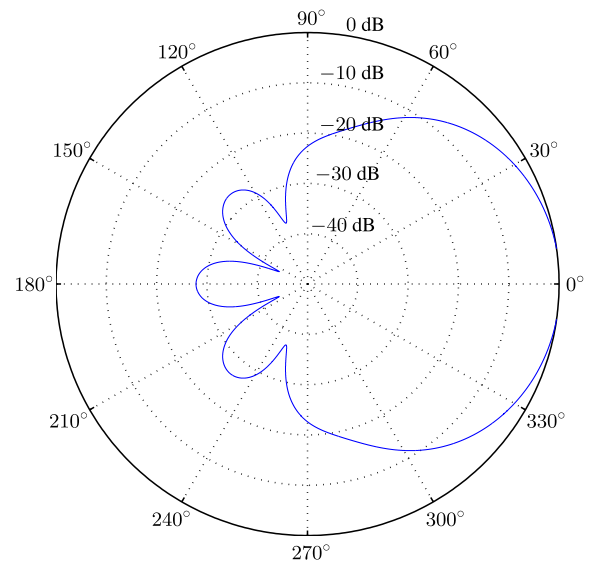


Fig. 27. Pattern of the robust third-order DMA designed with the Jacobi-Anger expansion. $M = 10$, $\delta = 1.5$ cm and $f = 1$ kHz.

The expectations in (74)–(76) can be computed as

$$E[\cos(2\theta)] = \frac{1}{\pi} \int_0^\pi \cos(2\theta) d\theta = 0, \quad (77)$$

$$E[\cos(2\theta) \cos \theta] = \frac{1}{\pi} \int_0^\pi \cos(2\theta) \cos \theta d\theta = \frac{1}{\pi} \int_0^\pi \frac{1}{2} [\cos \theta + \cos(3\theta)] d\theta = 0, \quad (78)$$

$$E[\cos^2(2\theta)] = \frac{1}{\pi} \int_0^\pi \cos^2(2\theta) d\theta = \frac{1}{\pi} \int_0^\pi \frac{1}{2} [1 + \cos(4\theta)] d\theta = \frac{1}{2}, \quad (79)$$

$$E[e^{j\varpi_m \cos \theta} \cos(2\theta)] = \frac{1}{\pi} \int_0^\pi e^{j\varpi_m \cos \theta} \cos(2\theta) d\theta = I_2(j\varpi_m) = -J_2(\varpi_m). \quad (80)$$

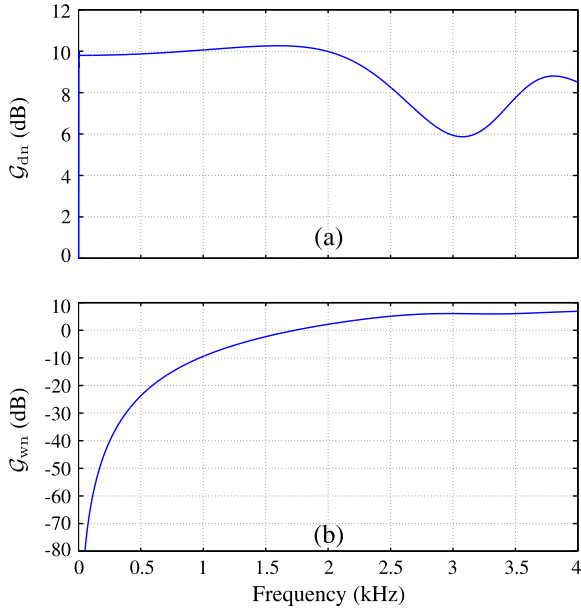


Fig. 28. SNR gains of the robust third-order DMA designed with the Jacobi–Anger expansion: (a) DF and (b) WNG. $M = 10$ and $\delta = 1.5$ cm.

Plugging (66)–(69), (77)–(80) into (74)–(76), we get

$$c_0 = J_0(\varpi_m), \tag{81}$$

$$c_1 = 2J_1(\varpi_m). \tag{82}$$

$$c_2 = -2J_2(\varpi_m). \tag{83}$$

Therefore, the optimal second-order approximation of $e^{j\varpi_m \cos \theta}$ is

$$e^{j\varpi_m \cos \theta} = J_0(\varpi_m) + 2J_1(\varpi_m) \cos \theta - 2J_2(\varpi_m) \cos(2\theta). \tag{84}$$

Using the same methodology, we can find that the optimal N th-order approximation of $e^{j\varpi_m \cos \theta}$ is

$$e^{j\varpi_m \cos \theta} = J_0(\varpi_m) + 2 \sum_{n=1}^N J_n(\varpi_m) \cos(n\theta). \tag{85}$$

It is clear that the previous expression corresponds to the Jacobi–Anger expansion [Eq. (24)], verifying that the Jacobi–Anger expansion is the optimal approximation of $e^{j\varpi_m \cos \theta}$ in the MSE sense.

Appendix B

In this section, we will demonstrate that the white noise gain of the proposed DMAs is generally an increasing function of M , the number of microphones. In Fig. 29, one can see that the white noise gain improves when M increases, confirming the merit of using more microphones and the minimum-norm filters in combating the white noise amplification problem. However, when M is large (e.g., M is greater than 10 in the first-order DMA), the additional performance gain is not significant while the practical cost can be. In the following, we will take the first-order DMA as an example and present more explanations.

We recall that the white noise gain of the first-order DMA has the form:

$$\mathcal{G}_{\text{wn}}[\mathbf{h}(\omega)] = \frac{|\mathbf{h}^H(\omega)\mathbf{d}(\omega, 0)|^2}{\mathbf{h}^H(\omega)\mathbf{h}(\omega)} = \frac{|\mathcal{B}_{M,1}[\mathbf{h}(\omega), 0]|^2}{\mathbf{h}^H(\omega)\mathbf{h}(\omega)}, \tag{86}$$

where $\mathcal{B}_{M,1}[\mathbf{h}(\omega), 0]$ is the beampattern of the first-order DMA at $\theta = 0$, and it is an approximation of $\mathcal{B}_M[\mathbf{h}(\omega), 0]$. Since the beampattern of the first-order DMA is frequency independent, i.e.,

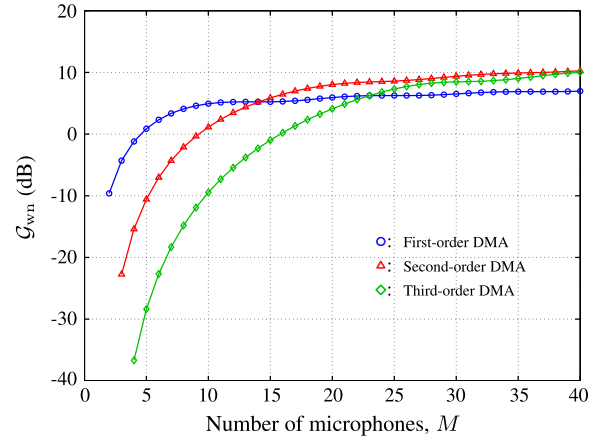


Fig. 29. White noise gain of the DMAs designed with the Jacobi–Anger expansion as a function of the number of microphones. $\delta = 1.5$ cm and $f = 1$ kHz.

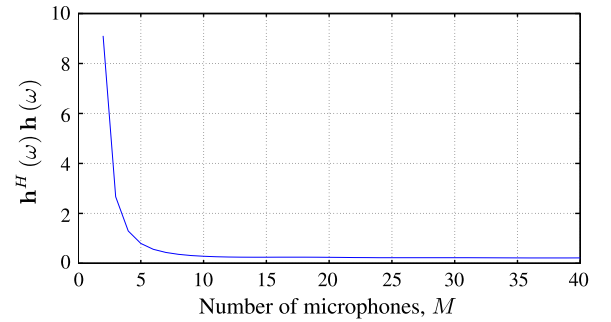


Fig. 30. The denominator of the white noise gain with the first-order DMA based on the Jacobi–Anger expansion (supercardioid). $\delta = 1.5$ cm and $f = 1$ kHz.

$$\mathcal{B}_{M,1}[\mathbf{h}(\omega), \theta] = \mathcal{B}_{C,1}(\theta) = b_0 + b_1 \cos \theta, \tag{87}$$

we have

$$\mathcal{B}_{M,1}[\mathbf{h}(\omega), 0] = b_0 + b_1. \tag{88}$$

Substituting (88) into (86), we can rewrite the white noise gain of the first-order DMA as

$$\mathcal{G}_{\text{wn}}[\mathbf{h}(\omega)] = \frac{|b_0 + b_1|^2}{\mathbf{h}^H(\omega)\mathbf{h}(\omega)}. \tag{89}$$

Using (36) and (37), we can express the denominator of the white noise gain as

$$\mathbf{h}^H(\omega)\mathbf{h}(\omega) = \sum_{m=1}^M |H_m(\omega)|^2 = b_0^2 + \frac{b_1^2}{4} \frac{1}{\sum_{m=2}^M J_1^2(\varpi_m)} + \frac{b_1^2}{4} \frac{[\sum_{m=2}^M J_0(\varpi_m)J_1(\varpi_m)]^2}{[\sum_{m=2}^M J_1^2(\varpi_m)]^2}. \tag{90}$$

Fig. 30 shows that $\mathbf{h}^H(\omega)\mathbf{h}(\omega)$ is a decreasing function of M ($M \geq 2$) and, therefore, it can be deduced from (89) that the white noise gain of the first-order DMA is, in general, an increasing function of M ($M \geq 2$).

The results of the white noise gain for the second-order and third-order DMAs can be explained similarly, but since the equations are too lengthy, we do not present them here.

References

- [1] Brandstein M, Ward DB, editors. *Microphone arrays: signal processing techniques and applications*. Berlin, Germany: Springer-Verlag; 2001.
- [2] Huang Y, Benesty J, Chen J. *Acoustic MIMO signal processing*. Berlin, Germany: Springer-Verlag; 2006.
- [3] Elko GW, Meyer J. Microphone arrays. In: Benesty J, Sondhi MM, Huang Y, editors. *Springer handbook of speech processing*. Berlin, Germany: Springer-Verlag; 2008. p. 1021–41 [chapter 50].
- [4] Benesty J, Chen J, Huang Y. *Microphone array signal processing*. Berlin, Germany: Springer-Verlag; 2008.
- [5] Benesty J, Souden M, Huang Y. A perspective on differential microphone arrays in the context of noise reduction. *IEEE Trans Audio Speech Lang Process* 2012;20:699–704.
- [6] Benesty J, Chen J. *Study and design of differential microphone arrays*. Berlin, Germany: Springer-Verlag; 2012.
- [7] Elko GW. Superdirectional microphone arrays. In: Gay SL, Benesty J, editors. *Acoustic signal processing for telecommunication*. Boston, MA: Kluwer Academic Publishers; 2000. p. 181–237 [chapter 10].
- [8] Zhao L, Benesty J, Chen J. Design of robust differential microphone arrays. *IEEE/ACM Trans Audio Speech Lang Process* 2014;22:1455–66.
- [9] Olson HF. Gradient microphones. *J Acoust Soc Am* 1946;17:192–8.
- [10] Ellithorn HE, Wiggins AM. Antinoise characteristics of differential microphones. *Proc IRE* 1946:84–9.
- [11] Teutsch H, Elko GW. First- and second-order adaptive differential microphone arrays. In: *Proc IWAENC*; 2001.
- [12] Elko GW. Microphone array systems for hands-free telecommunication. *Speech Commun* 1996;20:229–40.
- [13] Buck M. Aspects of first-order differential microphone arrays in the presence of sensor imperfections. *Eur Trans Telecommun* 2002;13:115–22.
- [14] Ihle M. Differential microphone arrays for spectral subtraction. In: *Proc IWAENC*; 2003.
- [15] Abhayapala TD, Gupta A. Higher order differential-integral microphone arrays. *J Acoust Soc Am* 2010;127:EL227–33.
- [16] De Sena E, Hacıhabiboğlu H, Cvetković Z. On the design and implementation of higher-order differential microphones. *IEEE Trans Audio Speech Lang Process* 2012;20:162–74.
- [17] Uzkov AI. An approach to the problem of optimum directive antenna design. *Comptes Rendus (Doklady) de l'Academie des Sciences de l'URSS* 1946;LIII (1):35–8.
- [18] Abramowitz M, Stegun IA, editors. *Handbook of mathematical functions with formulas, graphs, and mathematical tables*. New York: Dover; 1970.
- [19] Gil A, Segura J, Temme NM. *Numerical methods for special functions*. Philadelphia: Society for Industrial and Applied Mathematics; 2007.
- [20] Colton D, Kress R. *Inverse acoustics and electromagnetic scattering theory*. Second Edition. Berlin, Germany: Springer-Verlag; 1998.
- [21] Cuyt A, Petersen VB, Verdonk B, Waadeland H, Jones WB. *Handbook of continued fractions for special functions*. Berlin, Germany: Springer-Verlag; 2008.